Study of second lightest neutralino $\tilde{\chi}_2^0$ spin measurement with ATLAS detector at LHC

M. Biglietti[a], I. Borjanovic[b], G. Carlino[a], F. Conventi[a,d], E. Gorini[b,c], A. Migliaccio[a,d], E. Musto[a,d], M. Primavera[c], S. Spagnolo[b,c], A. Ventura[c]

[a] *Sezione INFN, Napoli, Italy*

[b] *Dipartimento di Fisica - Università degli Studi, Lecce, Italy*

[c] *Sezione INFN, Lecce, Italy*

[d] *Dipartimento di Fisica - Università "Federico II", Napoli, Italy*

Abstract

One of the goals of the ATLAS experiment at the CERN Large Hadron Collider is to search for evidence of Supersymmetry (SUSY) signals. If SUSY would be discovered, it will be fundamental to measure the spin of the new particles in order to prove that they are indeed supersymmetric partners. Left-handed squark cascade decay to second lightest neutralino ($\tilde{\chi}_2^0$) which further decays to slepton can represent a good opportunity for SUSY particles' spin measurement. Assuming the neutralino spin to be 1/2, the invariant mass distributions of some detectable final products of the reactions have to be charge asymmetric. In the present work the detectability of this charge asymmetry is analysed in the stau-coannihilation region and in the bulk region of the minimal Supergravity parameter space allowed by the latest experimental constraints. The criteria used to isolate the decay chain of interest and to reject the background, coming from both Standard Model and different SUSY decay channels, are described as obtained by suitable optimizations on Monte Carlo samples produced with the ATLAS fast simulation. The estimates of the residual contributions to background and of the applied cut efficiencies are presented. Results on charge asymmetry are then shown and discussed.

1 Introduction

The Minimal Supersymmetric extension of the Standard Model (MSSM) [1] is one of the most promising candidates to describe the physics beyond the Standard Model. It has a huge number of free parameters which can be significantly reduced by assuming particular mediation mechanism of the supersymmetry (SUSY) breaking. Most of Monte Carlo studies of the Large Hadron Collider (LHC) potential are performed within minimal Supergravity (mSUGRA) model. Within the mSUGRA framework masses, mixings and decays of all SUSY and Higgs particles are determined in terms of four input parameters and a sign: the common mass m_0 of scalar particles at the grand unification scale, the common fermion mass $m_{1/2}$, the common trilinear coupling A_0, the ratio of the Higgs vacuum expectation values $\tan\beta$ and the sign of the supersymmetric Higgs mass parameter μ. In mSUGRA with R-parity conserved, the lightest supersymmetric particle (lightest neutralino $\tilde{\chi}_1^0$) is a suitable candidate for Dark Matter. The mSUGRA parameter space is highly constrained by the latest experimental data: WMAP measurements of the density of non-barionic Dark Matter, LEP lower limits on SUSY masses, branching ratio measurements for $b \rightarrow s\,\gamma$ decay from BELLE, CLEO and BABAR experiments and recent BNL measurements of muon anomalous magnetic moment [2]. Discovery of the SUSY particles with TeV masses will be possible at the Large Hadron Collider for the mSUGRA model. Once the signal of a physics beyond the Standard Model is seen, it will be fundamental to measure properties of new particles, like spin, in order to prove that they are indeed supersymmetric partners. The spin analysis method proposed by A. Barr [3] allows the discrimination of different hypotheses for spin assignments by measuring a charge asymmetry at the LHC. Some studies [4], [5] show that this method can also be used for the discrimination of SUSY from an Universal Extra Dimensions (UED) model which can mimick low energy SUSY at hadron colliders.

In this report two selected points inside stau-coannihilation and bulk regions of the allowed mSUGRA parameter space are considered. Fast simulation studies were performed in order to investigate the feasibility of supersymmetric particles' spin measurement by using the method proposed in [3].

In Sect. 2 the strategy applied for spin measurement is described, for which the cascade decay of the left-handed squark $\tilde{q}_L$ has been used. Experimental effects which dilute asymmetry measurement are introduced and discussed. Features of the studied mSUGRA points and properties of $\tilde{q}_L$ cascade decay for these points are described in Sect. 3. In Sect. 4 all Monte Carlo data sets and simulation/reconstruction tools used for this analysis are specified. The MC truth level distributions of invariant masses and the charge asymmetries are also shown. The analysis procedure is presented in Sect. 5 including event selection, background study and reconstruction of invariant masses. The statistical methods used for estimating charge asymmetries and results on their detectability are reported in Sect. 6. Sect. 7 is devoted to conclusions.

2 Spin measurement

The cascade decay of the $\tilde{q}_L$ (Fig. 1) to $\tilde{\chi}_2^0$ which further decays to slepton

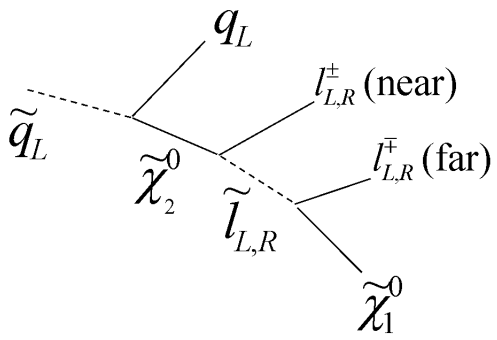

Fig. 1: Schematic view of left-handed squark decay. Lepton from $\tilde{\chi}_2^0$ decay is called *near*, lepton from $\tilde{l}_{L,R}$ decay is called *far*.

$$\tilde{q}_L \;\rightarrow\; \tilde{\chi}_2^0\, q \;\rightarrow\; \tilde{l}^{\pm}\, l^{\mp}\, q \;\rightarrow\; l^+\, l^-\, q\;\; \tilde{\chi}_1^0\,, \tag{2.1}$$

is very convenient for the supersymmetric particles' spin measurement [3]. Here the notations $\tilde{q}_L = \tilde{u}_L$, $\tilde{d}_L$, $\tilde{c}_L$, $\tilde{s}_L$ and $\tilde{l}$= $\tilde{e}_{L,R}$, $\tilde{\mu}_{L,R}$, $\tilde{\tau}_{1,2}$ are assumed. In the following, the first emitted lepton (the one from $\tilde{\chi}_2^0$ decay) is called *near*, and the one from slepton decay is called *far*, because it is emitted later.

In the MSSM, squarks and sleptons are spin-0 particles and their decays are spherically symmetric. The second lightest neutralino has spin 1/2 and the angular distribution of its decay products is not isotropic. When $\tilde{\chi}_2^0$ decays to right-handed slepton in the decay (2.1), the probability distribution functions for the invariant masses $m(ql^{near(\pm)})$ that the quark from the squark decay forms with the near lepton, are:

$$\frac{dP_1}{d\hat{m}} = 4\sin^3\frac{\theta^*}{2} = 4\hat{m}^3, \qquad \frac{dP_2}{d\hat{m}} = 4\sin\frac{\theta^*}{2}\cos^2\frac{\theta^*}{2} = 4\hat{m}(1-\hat{m}^2),$$

for $m(ql^{near(+)})$ and $m(ql^{near(-)})$, respectively. Here $\hat{m}$ is the invariant mass of quark and near lepton normalised to its maximum value: $\hat{m} = m(ql^{near})/m(ql^{near})^{max} = \sin\frac{\theta^*}{2}$ and θ^* is the angle between quark and near lepton in the $\tilde{\chi}_2^0$ rest frame. This leads to a charge asymmetry of the invariant masses $m(ql^{near(\pm)})$ [3]. Charge asymmetry is defined as

$$A = \frac{s^+ - s^-}{s^+ + s^-}, \qquad s^{\pm} = \frac{d\sigma}{dm(ql^{\pm})}\,. \tag{2.2}$$

The invariant mass of quark and far lepton $m(ql^{far})$ also possesses some small charge asymmetry from the relativistic boost [5]. It is not always possible to distinguish experimentally near from far lepton, as, for example, in the case of the bulk point, so charge asymmetry of invariant mass of quark and lepton $m(ql)$ can be measured including contributions from both near and far leptons. This effect can dilute measurement of charge asymmetry.

In the left-handed anti-squark cascade decay, the asymmetry in the corresponding $m(\bar{q}l)$ charge distributions is the same as the asymmetry in $m(ql)$ from $\tilde{q}_L$ decay, but with opposite sign [6]. The charge of the squark (quark) can not be measured and it is not possible to distinguish quark from anti-quark. However, at a proton-proton collider like the LHC, more squarks than anti-squarks will be produced, since the quark Parton Distribution Function is larger than that of the antiquark, due to the presence of the valence quarks. This leads to a significant lepton charge asymmetry. Denoting $\tilde{q}$ ($\bar{\tilde{q}}$) the number of squarks (antisquarks) produced, the significance of this asymmetry [7] can be defined as:

$$S = \frac{\tilde{q} - \bar{\tilde{q}}}{\sqrt{\tilde{q} + \bar{\tilde{q}}}} \cdot \sqrt{ab}$$

where a is the detector acceptance and b the branching ratio of the selected decay chain. Assuming that the acceptance is independent of the chosen mSUGRA point, for a given integrated luminosity, S will depend, all over mSUGRA parameter space, on SUSY production cross section, on the ratio $\tilde{q}/\bar{\tilde{q}}$ and on b.

3 SUSY production and kinematics

3.1 Stau-coannihilation point

One of the allowed regions in the mSUGRA parameter space is the stau-coannihilation region. In this region the lightest stau slepton $\tilde{\tau}_1$ is slightly heavier than the $\tilde{\chi}_1^0$ and acceptable relic density of cold Dark Matter is obtained through enhanced stau-neutralino coannihilation processes. The point selected for study, so called SU1 point, has parameters:

$$m_0 = 70 \text{ GeV}, \quad m_{1/2} = 350 \text{ GeV}, \quad A_0 = 0 \text{ GeV}, \quad tan\beta = 10, \quad sgn\mu = + \,.$$

The lightest neutralino is purely bino. The LO cross section for all SUSY production is $\sigma = 7.8$ pb and it is dominated by the production of squarks and gluinos. The heaviest SUSY particle is gluino $\tilde{g}$ with mass $m(\tilde{g}) = 832$ GeV and the lightest SUSY particle is $\tilde{\chi}_1^0$, with a mass of 137 GeV.

One/two left-handed squark/s is/are directly produced in 32%/8% of all SUSY events and can also be indirectly originated in 20% of all gluino decays. Cross

sections for $\tilde{q}_L$ and $\tilde{g}$ productions are:

$$\sigma(\tilde{q}_R\tilde{g}) = 1.8\ pb\ , \quad \sigma(\tilde{q}_L\tilde{g}) = 1.6\ pb\ ,$$
$$\sigma(\tilde{q}_L\tilde{q}_R) = 0.9\ pb\ , \quad \sigma(\tilde{q}_L\tilde{q}_L) = 0.7\ pb\ ,$$
$$\sigma(\tilde{g}\tilde{g}) = 0.6\ pb\ , \quad \sigma(\tilde{q}_L\tilde{\chi}_2^0) = 0.2\ pb\ .$$

Since the $\tilde{\chi}_2^0$ is heavier than both left-handed and right-handed sleptons ($\tilde{l}_{L,R}$, l=e,μ), in the cascade decay of $\tilde{q}_L$ it can decay to both $\tilde{l}_L$ and $\tilde{l}_R$:

$$\tilde{q}_L \ \rightarrow\ \tilde{\chi}_2^0\, q \ \rightarrow\ \tilde{l}_{L,R}^{\pm} l^{\mp}\, q \ \rightarrow\ l^+\, l^-\, q\ \tilde{\chi}_1^0\ . \tag{3.1}$$

Since identification of the hadronic tau decays has a strong dependence on the detector performance, thus needing a detailed and complete ATLAS simulation to be studied, decays of $\tilde{\chi}_2^0$ to stau sleptons are not analysed in this report.

Masses of the particles involved in the $\tilde{q}_L$ decay are $m(\tilde{u}_L, \tilde{c}_L) = 760$ GeV, $m(\tilde{d}_L, \tilde{s}_L) = 765$ GeV, $m(\tilde{\chi}_2^0) = 264$ GeV, $m(\tilde{l}_L) = 255$ GeV, $m(\tilde{l}_R) = 154$ GeV and $m(\tilde{\chi}_1^0) = 137$ GeV, where $\tilde{l}_{L,R} = \tilde{e}_{L,R}$, $\tilde{\mu}_{L,R}$ and $l = e, \mu$. Main characteristic of SU1 point is that the mass difference between $\tilde{\chi}_2^0$ and $\tilde{l}_L$ is small ($m(\tilde{\chi}_2^0) - m(\tilde{l}_L) \approx 10$ GeV): as a consequence the near lepton has low p_T in the $\tilde{\chi}_2^0 \rightarrow \tilde{l}_L\, l$ decay. Similarly, the small mass difference between $\tilde{l}_R$ and $\tilde{\chi}_1^0$ ($m(\tilde{l}_R) - m(\tilde{\chi}_1^0) \approx 20$ GeV), implies low values for far lepton's p_T in $\tilde{\chi}_2^0 \rightarrow \tilde{l}_R\, l$ decays. As a consequence, near and far leptons are distinguishable in SU1 point.

Branching ratios for the involved decays are:

$$BR(\tilde{q}_L \rightarrow q\tilde{\chi}_2^0) = 32\ \%, \quad BR\ (\ \tilde{\chi}_2^0\ \rightarrow\ \tilde{l}_L\, l\ ) = 6\ \%,$$
$$BR\ (\ \tilde{\chi}_2^0\ \rightarrow\ \tilde{l}_R\, l\ ) = 3\ \%, \quad BR(\tilde{l}_{L,R} \rightarrow \tilde{\chi}_1^0\, l) = 100\ \%.$$

Decay (3.1) represents about 1.6% of all SUSY production. Taking into account this value, and the fact that observability of charge asymmetry is favoured by a ratio of about 3.5 in the $\tilde{q}/\bar{\tilde{q}}$ production yield, for a fixed integrated luminosity of 100 fb^{-1}, the calculation of the significance provides $S \sim 50$.

Starting from the three detectable particles l^+, l^-, q (where quark hadronizes to jet) in the final state of the $\tilde{q}_L$ decay (3.1) four invariant masses can be formed: $m(ll)$, $m(qll)$, $m(ql^{near})$ and $m(ql^{far})$. For each of them, expressions and corresponding values (for $\tilde{q}_L$= $\tilde{d}_L$, $\tilde{s}_L$) for kinematic maxima are given by equations (3.2)-(3.5) [8]:

$$m(ll)^{max} = \left[\frac{(M^2_{\tilde{\chi}_2^0} - M^2_{\tilde{l}_{L,R}})(M^2_{\tilde{l}_{L,R}} - M^2_{\tilde{\chi}_1^0})}{M^2_{\tilde{l}_{L,R}}}\right]^{1/2} =$$
$$= 56\ \text{GeV}\ (\tilde{l}_L),\ \ 98\ \text{GeV}\ (\tilde{l}_R)\ , \tag{3.2}$$
$$m(qll)^{max} = \left[\frac{(M^2_{\tilde{q}_L} - M^2_{\tilde{\chi}_2^0})(M^2_{\tilde{\chi}_2^0} - M^2_{\tilde{\chi}_1^0})}{M^2_{\tilde{\chi}_2^0}}\right]^{1/2} =$$
$$= 614\ \text{GeV}\ (\tilde{l}_L, \tilde{l}_R)\ , \tag{3.3}$$

$$m(ql^{near})^{max} = \left[\frac{(M^2_{\tilde{q}_L} - M^2_{\tilde{\chi}^0_2})(M^2_{\tilde{\chi}^0_2} - M^2_{\tilde{l}_{L,R}})}{M^2_{\tilde{\chi}^0_2}}\right]^{1/2} =$$

$$= 181 \text{ GeV } (\tilde{l}_L), \quad 583 \text{ GeV } (\tilde{l}_R)\,, \tag{3.4}$$

$$m(ql^{far})^{max} = \left[\frac{(M^2_{\tilde{q}_L} - M^2_{\tilde{\chi}^0_2})(M^2_{\tilde{l}_{L,R}} - M^2_{\tilde{\chi}^0_1})}{M^2_{\tilde{l}_{L,R}}}\right]^{1/2} =$$

$$= 329 \text{ GeV } (\tilde{l}_R), \quad 606 \text{ GeV } (\tilde{l}_L)\,. \tag{3.5}$$

3.2 Bulk point

The bulk region is one of the allowed regions of mSUGRA parameter space. An acceptable relic density of cold Dark Matter is obtained thanks to the lightest neutralino annihilation processes via t-channel slepton exchange. The point considered for study, so called SU3 point, has parameters:

$$m_0 = 100 \text{ GeV}, \quad m_{1/2} = 300 \text{ GeV}, \quad A_0 = -300 \text{ GeV}, \quad tan\beta = 6, \quad sgn\mu = +\,.$$

The lightest neutralino is mostly bino. Total SUSY LO cross section is $\sigma = 19.3$pb and is dominantly characterised by gluino and squark production. In SU3 point gluino is the heaviest SUSY particle ($m(\tilde{g}) = 717$ GeV) while the lightest particle is $\tilde{\chi}^0_1$ ($m(\tilde{\chi}^0_1) = 118$ GeV).

Left-handed squarks occur in 67% of all SUSY events, and can be produced either directly or from gluino decay ($BR(\tilde{g} \rightarrow \tilde{q}_L q) = 23\%$). Cross sections for gluino and squark direct production are:

$$\sigma(\tilde{q}_R\tilde{g}) = 4.5\ pb\,, \quad \sigma(\tilde{q}_L\tilde{g}) = 4.4\ pb\,,$$
$$\sigma(\tilde{q}_L\tilde{q}_R) = 2.1\ pb\,, \quad \sigma(\tilde{q}_L\tilde{q}_L) = 1.7\ pb\,,$$
$$\sigma(\tilde{g}\tilde{g}) = 1.5\ pb\,, \quad \sigma(\tilde{q}_L\tilde{\chi}^0_2) = 0.2\ pb\,.$$

Differently from the SU1 point, the mass of the second lightest neutralino ($m(\tilde{\chi}^0_2) = 219$ GeV) is smaller than $\tilde{l}_L$ mass ($m(\tilde{l}_L) = 230$ GeV). As a consequence, decays of $\tilde{\chi}^0_2$ to left-handed sleptons are forbidden and only decays to right-handed sleptons are allowed in the $\tilde{q}_L$ cascade decay (3.8% of all SUSY production):

$$\tilde{q}_L \rightarrow \tilde{\chi}^0_2\, q \rightarrow \tilde{l}^{\pm}_R\, l^{\mp}\, q \rightarrow l^+\, l^-\, q\ \tilde{\chi}^0_1\,. \tag{3.6}$$

Masses and branching ratios of particles from decay (3.6) are:

$$m(\tilde{d}_L, \tilde{s}_L) = 636 \text{ GeV}, \quad m(\tilde{u}_L, \tilde{c}_L) = 631 \text{ GeV},$$
$$m(\tilde{\chi}^0_2) = 219 \text{ GeV}, m(\tilde{l}_R) = 155 \text{ GeV}, m(\tilde{\chi}^0_1) = 118 \text{ GeV},$$
$$BR(\tilde{q}_L \rightarrow q\tilde{\chi}^0_2) = 32\ \%,\ BR(\tilde{\chi}^0_2 \rightarrow \tilde{l}_R\, l) = 18\%,\ BR(\tilde{l}_R \rightarrow \tilde{\chi}^0_1\, l) = 100\ \%,$$

where $\tilde{l}_R = \tilde{e}_R,\ \tilde{\mu}_R$ and $l = e, \mu$.

In SU3 point, the squarks/anti-squarks production ratio is about 3. Despite this lower value with respect to SU1, the larger production cross section and the higher branching ratios of the involved processes, for an integrated luminosity of 100 fb^{-1}, bring the significance S to ~ 110.

Endpoints for the invariant masses $m(ll)$, $m(qll)$, $m(ql^{near})$, $m(ql^{far})$ given by equations (3.2)-(3.5) for $\tilde{q}_L$= $\tilde{d}_L$, $\tilde{s}_L$ are:

$$m(ll)^{max} = 100 \text{ GeV}, \tag{3.7}$$
$$m(qll)^{max} = 503 \text{ GeV}, \tag{3.8}$$
$$m(ql^{near})^{max} = 420 \text{ GeV}, \tag{3.9}$$
$$m(ql^{far})^{max} = 389 \text{ GeV}. \tag{3.10}$$

It is not possible to experimentally distinguish near from far lepton in the bulk point. For this reason, when studying asymmetries (see Sect. 5), the invariant mass of quark and lepton $m(ql)$ is reconstructed summing contributions from near and far leptons, $m(ql^{near})$ and $m(ql^{far})$.

4 Monte Carlo simulations

4.1 MC samples

Events were generated with HERWIG 6.505 [9, 10, 11], by using the ISAWIG [12] interface with mass spectra and decay rates of supersymmetric particles given by ISAJET 7.69 and ISAJET 7.64 [13] for SU1 and SU3 points, respectively. SUSY samples corresponding to integrated luminosities $L = 100$ fb^{-1} (out of an overall sample of 220 fb^{-1}) for SU1 point and $L = 30$ fb^{-1} for SU3 point were analysed: this statistics was obtained by adding all the available official Rome productions [14] and privately generated samples, produced at Tier 2 farm facility in Napoli (Italy). All samples have been simulated according to the standard ATLAS rules for MC production, thus ensuring their statistical uncorrelation.

Fast simulation studies on the most relevant Standard Model (SM) background have been also performed. In particular the processes considered in this report are: $t\bar{t}$ + N partons, W + N partons, Z + N partons [15], produced with Alpgen 2.0.5 [16]. Generated events were passed through fast simulation package of ATLAS detector, ATLFAST (AtlFast-00-01-74) [17]. AOD files were produced with ATHENA 10.0.4. Analysis on AOD files was performed with SUSYPlot package (SUSYPhysAlgs-00-04-02).

In ATLFAST simulation leptons were required to have transverse momentum $p_T > 6$ (5) GeV for muons (electrons), pseudorapidity $|\eta| < 2.5$ and deposited transverse energy $E_T^{isol} < 10$ GeV within a cone $\Delta R = 0.2$, in order to be marked as isolated. Jets were reconstructed by a jet-cone algorithm with $\Delta R = 0.4$. Minimum jet p_T was 15 GeV in $|\eta| < 5$. The final efficiency of the whole event selection

procedure described in Sect. 5.3 includes the contribution of the ATLFAST cuts listed above.

While ATLFAST tries to reproduce the main features of a *full* simulation, some important effects are actually left out [17], [18]: no pile-up is included, the effect of the underlying event is probably underestimated, no wrong charge assignment is simulated and, most of all, some misidentification processes, related to detector effects, in which a jet is taken as a lepton, are not simulated, regardless of the momentum value and of the lepton flavor. However, especially due to the low momenta of the leptons involved in the signal events, other processes can provide background sources of "non-signal" (and mostly non isolated) electrons or muons [19]: e.g. electrons coming from π^0 Dalitz decays or from semileptonic decays of B and D mesons, muons from $\pi^{\pm}$ decays on flight and from semileptonic B and D decays. In particular, the semileptonic decay contributions become large when the lepton isolation requirements are loosened.

The final background contamination estimated in this analysis (see Sect. 5.2) includes all contributions coming both from physics processes (SM or SUSY) involving pairs of isolated leptons and from misidentification processes in which leptons from hadronic particle decays or from jets, passing cuts, are regarded as signal ones. In ATLFAST, the number of leptons from hadronic particles or jets over the whole number of reconstructed leptons has been found to be 0.6% for electrons and 0.2% for muons, over the full lepton p_T range. The effect of this contamination on the charge asymmetry has been estimated for the SU3 point in this scenario, and also in the more pessimistic case in which the contribution of such leptons has been multiplied up to a factor three (see Sect. 6).

4.2 Charge asymmetries at MC truth level

This section considers MC truth level distributions for the SU1 and SU3 points. In all MC truth level plots shown here, q and $\bar{q}$ are treated as indistinguishable. Moreover, to take correctly into account the radiation emission mechanism from partons implemented in HERWIG, the components of the quark 4-momentum have been assigned the values provided in the corresponding Monte Carlo jet (JetTruth reconstruction algorithm). This explains tails after the endpoints values in the invariant mass distributions involving quarks.

As already discussed in Sect. 3.1, in SU1 point near and far leptons are distinguishable with high probability according to their p_T, whether they come from $\tilde{l}_L$ or $\tilde{l}_R$. This is evident in Fig. 2, where the p_T distributions of the near and far leptons are superimposed and compared for the two cases specified above.

Endpoints of $m(ll)$ and $m(qll)$ mass distributions (3.2-3.3) and (3.7-3.8), for SU1 and SU3 points respectively, are clearly visible in Figs. 3 and 4.

Some examples of lepton-quark invariant mass distributions, with positively and negatively charged leptons superimposed, are illustrated in Fig. 5 for SU1 and SU3 points respectively.

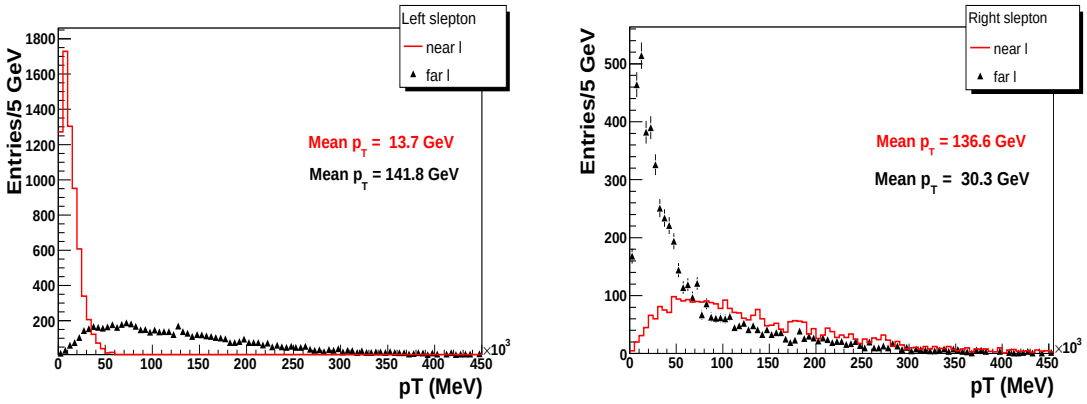

Fig. 2: p_T distributions at MC truth level in SU1 for near (in red) and far (in black) leptons in the chains involving $\tilde{l}_L$ (on the left) and $\tilde{l}_R$ (on the right).

Charge asymmetries of $m(ql)$ distributions at MC truth level are shown in Figs. 6 and 7. The shapes of these asymmetries, except in the case of far lepton from a left-handed slepton decay in SU1, are clearly inconsistent with a constant zero value (superimposed line in the plots). This demonstrates that, at parton level, asymmetries are still evident even after the diluting effects due to the presence of $\bar{\tilde{q}}_L$ and, in the SU3 case, also due to the undistinguishability of near/far leptons. Charge asymmetry is detectable with smaller statistics for the SU3 case, since cross sections and branching ratios for decay (3.6) are larger (despite the lower $\tilde{q}/\bar{\tilde{q}}$ ratio and the impossibility to distinguish near/far leptons). Concerning SU1 point, in the analysis described in the following, emphasis will be given only to $m(ql^{near})$ in the $\tilde{l}_L$ decay chain, which represents the case with the most enhanced asymmetry already at MC truth level. The method used to determine the confidence level of observing a zero charge asymmetry is described in Sect. 6.

5 Analysis

5.1 Event signature

SUSY events are dominated by the production of gluinos and squarks, which decay through one or more steps to the Lightest SUSY Particle (LSP), which is stable, weakly interacting and escapes from detection. A typical final state signature of $\tilde{q}_L$ cascade decays (3.1) and (3.6) is given by:

- large missing transverse energy,
- two same flavor opposite sign (SFOS) leptons,

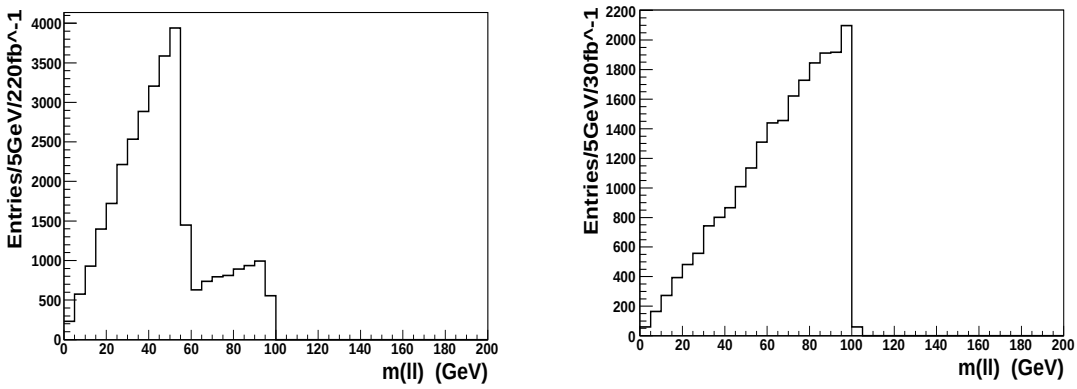

Fig. 3: Dilepton invariant mass distributions at MC truth level for SU1 (on the left) and SU3 (on the right).

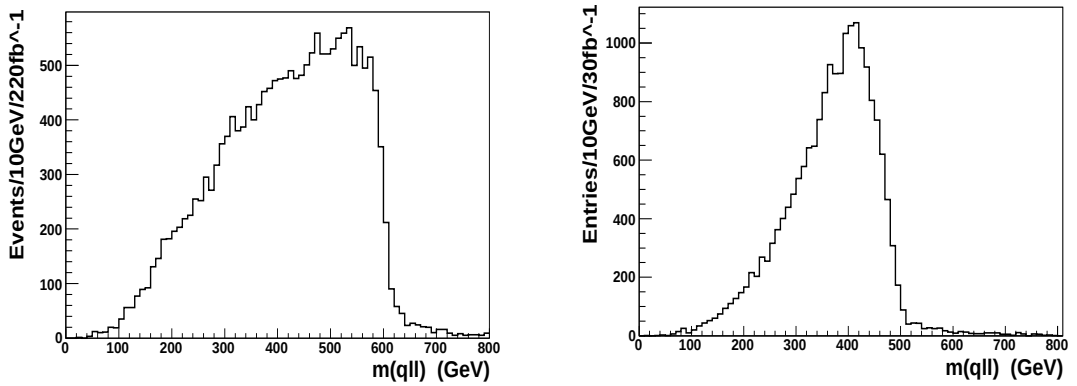

Fig. 4: $m(qll)$ distributions at MC truth level for SU1 (on the left) and SU3 (on the right).

- high-p_T jets from the left-handed squark decay and from the decay of squark/gluino produced with $\tilde{q}_L$.

5.2 Background

Both SM and SUSY processes can mimick the final state signature of $\tilde{q}_L$ decay chain described above. Background can be classified as irreducible or reducible, depending on whether the two SFOS leptons (e^+e^-, $\mu^+\mu^-$) in the event are correlated or not, respectively. An example of correlated SFOS leptons are e^+e^- or $\mu^+\mu^-$ from Z decay. On the other hand, uncorrelated SFOS leptons originate from two independent decays in the event. In the latter case the number of events with two uncorrelated SFOS leptons should be equal to the number of events with two opposite flavor op-

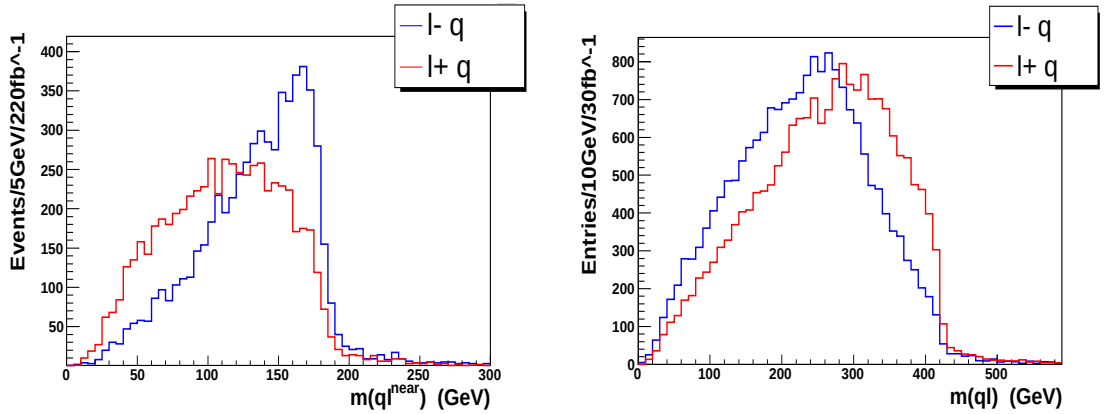

Fig. 5: Lepton-quark invariant mass distributions at MC truth level. Masses formed with positive and negative leptons are superimposed. Left: using the near lepton from the chain involving $\tilde{l}_L$ in SU1 point. Right: using both near and far leptons in SU3 point.

posite sign (OFOS) leptons ($e^{\pm}\mu^{\mp}$) and the corresponding dilepton invariant mass distributions should be identical. Consequently, reducible background can be suppressed by applying SFOS-OFOS subtraction ($e^+e^- + \mu^+\mu^- - e^{\pm}\mu^{\mp}$) on invariant mass distributions. When applying this subtraction the different detection efficiencies of electrons and muons as well as their dependence on parameters like p_T, η and ϕ must be taken into account by means of a weighting factor $\beta = \epsilon_\mu/\epsilon_e$, to be suitably parameterised, thus providing $\beta^2 e^+e^- + \mu^+\mu^- - \beta e^{\pm}\mu^{\mp}$. Since no reconstruction inside a realistic detector is simulated in ATLFAST, isolated electron and muon identification efficiencies are close to 1. In the following the lepton efficiency is assumed to be the same for electrons and muons (about 98.5%, $\beta = 1$) and flat over the full p_T range.

The main Standard Model background process is $t\bar{t}$ + jets production. Actually, because of the underlying event, pile-up, detector effects and misidentification processes like those described in Sect. 4, other SM processes like W/Z + jets can be also considered as sources of background.

The SM background sample analysed in this note is composed only by the processes described in Sect. 4.1. It can be significantly removed with hard kinematic cuts on missing transverse energy, isolation, number of jets and p_T of jets. After such cuts only a small fraction of $t\bar{t}$ + jets events survive (see Sect. 5.3), which are furtherly suppressed by applying SFOS-OFOS subtraction.

SUSY background is the dominant background, as will be shown in Table 1. In both SU1 and SU3 points, sources of irreducible background are: Z bosons produced in the decay of heavier gauginos decaying leptonically, directly produced $\tilde{\chi}_2^0$, and $\tilde{\chi}_2^0$ produced indirectly from stop, sbottom or heavier gaugino decays. Uncorrelated leptons can originate from $\tilde{\chi}_1^{\pm}$ chargino decays or from $\tilde{\chi}_2^0 \rightarrow \tilde{\tau}_1\tau$ decay.

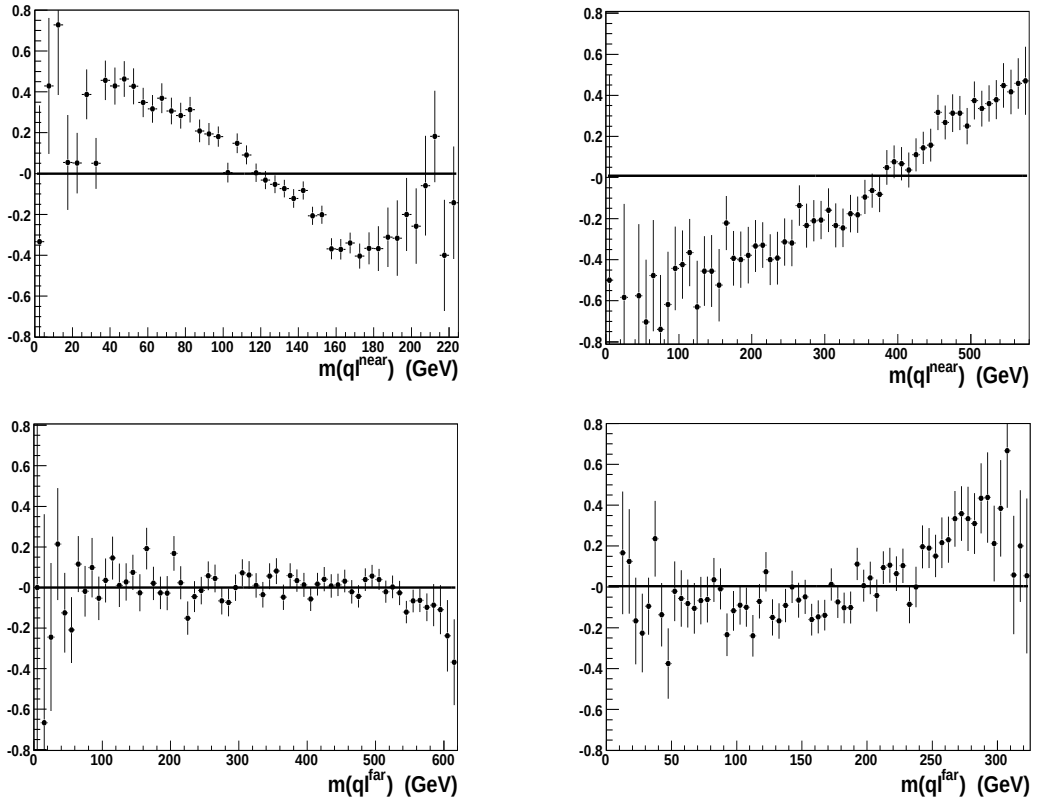

Fig. 6: $m(ql)$ charge asymmetries at MC truth level in SU1 point for an integrated luminosity of 220 fb^{-1}. Plots on the left (right) correspond to the chain involving $\tilde{l}_L$ ($\tilde{l}_R$).

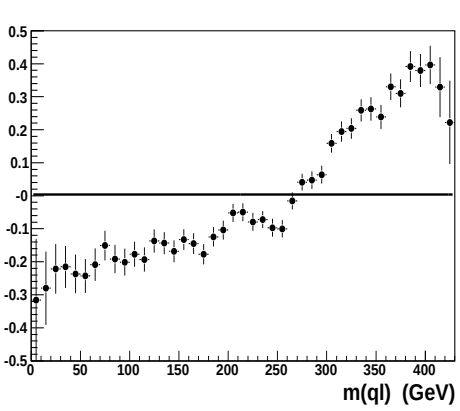

Fig. 7: $m(ql)$ charge asymmetry at MC truth level in SU3 point for an integrated luminosity of 30 fb^{-1}.

The reducible SUSY background with two uncorrelated leptons is removed with SFOS-OFOS subtraction.

5.3 Event selection

SUSY events can be separated from the SM background requiring the presence of large missing transverse energy and energetic hadronic jets.

In order to separate signal from SM background the following *preselection* cuts were applied for both SU1 and SU3 events:

- missing transverse energy $E_T^{miss} > 100$ GeV,
- at least four jets with transverse momentum $p_T(j_1) > 100$ GeV and $p_T(j_2, j_3, j_4) > 50$ GeV.

The E_T^{miss} distributions in all SUSY and SM events are shown in Fig. 8 for SU1 and SU3 points where the SUSY events have been filtered according to the same standard cuts at the parton level reported in [15] and applied to the SM samples.

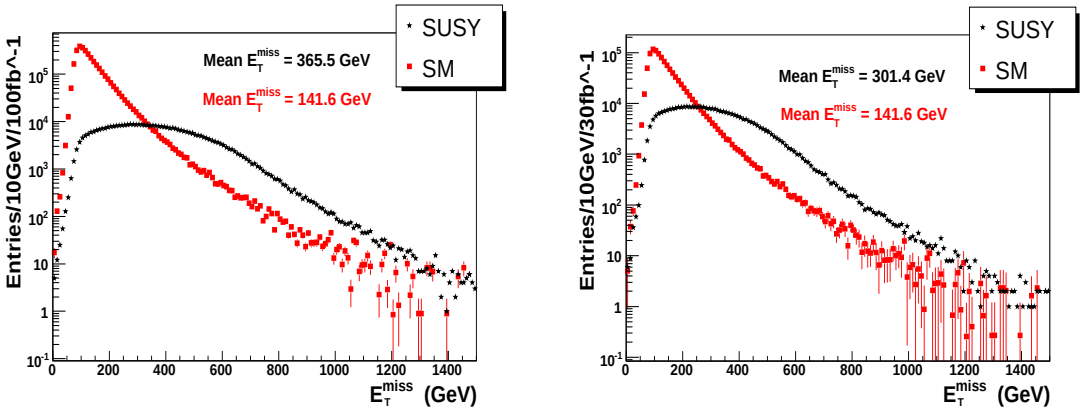

Fig. 8: Missing transverse energy distribution for SUSY events (in black) and SM background (in red) for SU1 (on the left) and SU3 (on the right) points.

The p_T distributions of the four most energetic jets for SUSY and SM events are shown in Fig. 9 for the SU1 point. On both SU1 and SU3 points, the preselection cuts previously defined have been found to provide a reasonable compromise between a high signal selection efficiency and a low SM background contamination.

The following selection is applied to select dilepton events:

- exactly two SFOS leptons (with transverse momenta $p_T^{lepton} > 6$ GeV for SU1 point, and $p_T^{lepton} > 10$ GeV for SU3 point).

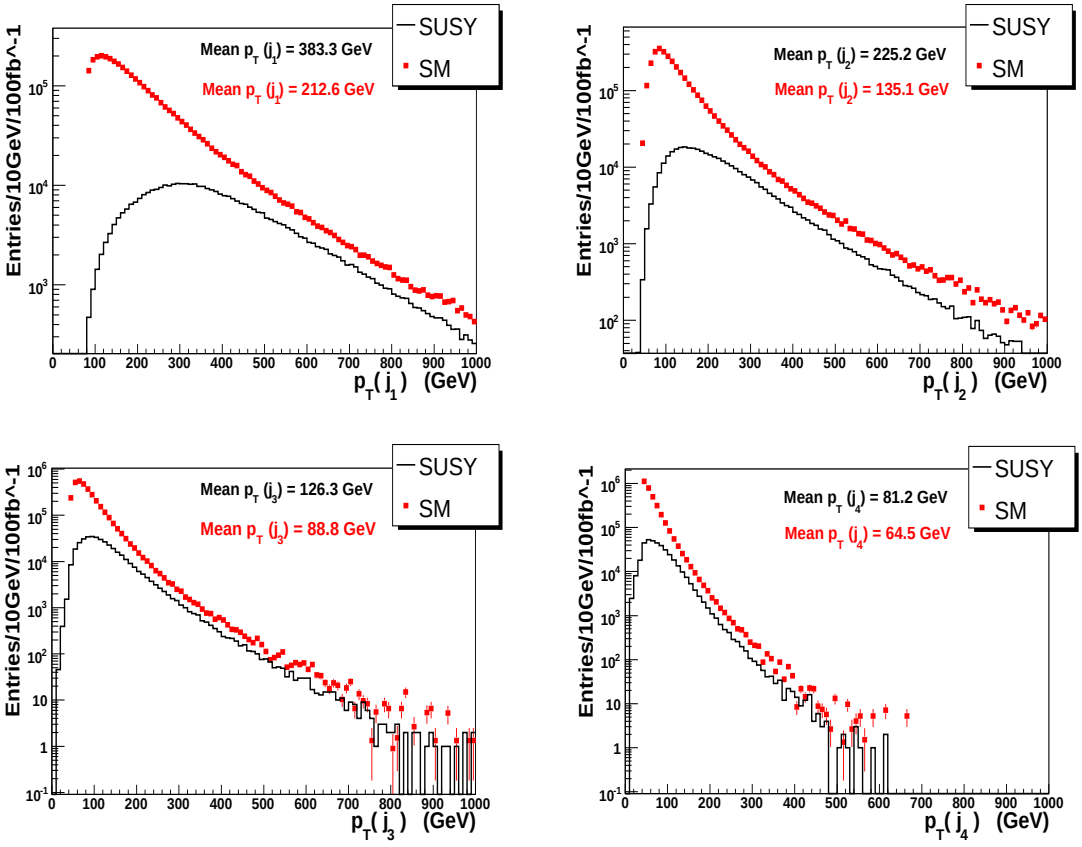

Fig. 9: Transverse momentum distributions of the four most energetic jets for SU1 events (in black) and SM background (in red).

Selection criteria on p_T of lepton are different for SU1 and SU3, owing to the different p_T spectra in these points. The requirement of exactly two SFOS leptons strongly suppresses both SUSY and SM background. Asking for a higher number of leptons in the event provides only a negligible gain in the signal yield (at most $\sim 10\%$) and introduces other sources of systematics due to combinatorics.

The following invariant masses are calculated after these selections:

- dilepton invariant mass $m(ll)$,
- lepton-lepton-jet invariant mass $m(jll)$,
- lepton-jet invariant masses $m(jl^+)$ and $m(jl^-)$,

where $l^\pm$ are the leptons and j is one of the two most energetic jets in the event (as described in more detail below). Events with two OFOS leptons are also selected and used to remove SUSY combinatorial background by performing the SFOS-OFOS subtraction on all mentioned mass distribution as already described in Sect. 5.2.

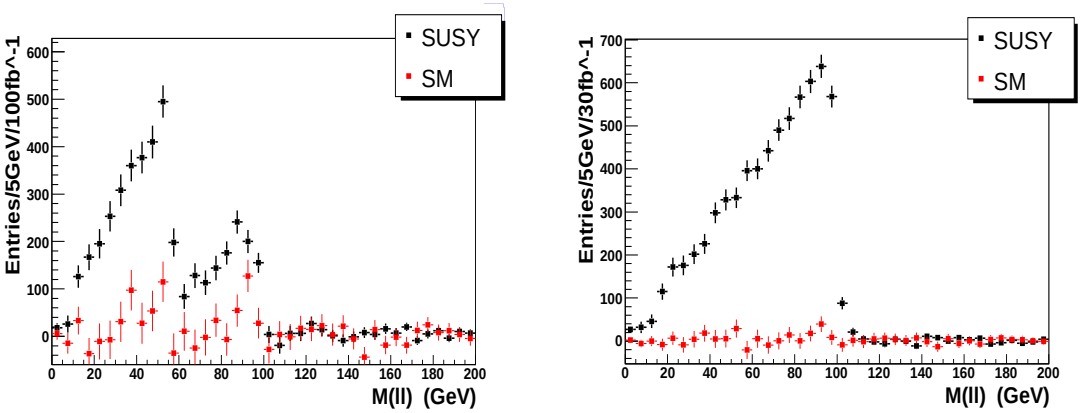

Fig. 10: Dilepton invariant mass after SFOS-OFOS subtraction for SUSY events (in black: SU1 on the left, SU3 on the right) and for SM events (in red).

In Fig. 10 are displayed dilepton invariant masses for SU1 and SU3 points and SM background, normalised to the integrated luminosity of each SUSY sample, after SFOS-OFOS subtraction. Apart from statistical fluctuations in the whole $m(ll)$ range, the only significant excess in terms of signal/background ratio (S/B) in the SM background distribution is observed in the region around 90 GeV, as expected, due to the irreducible contribution of the Z + jets sample. Reconstructed endpoints are at the expected positions for the considered SUSY points, and SUSY and SM background don't significantly deteriorate their sharpness, especially for SU3, in which the signal is enhanced by the high cross section and branching ratios for the decay of interest. Actually, in the high luminosity scenario required for the SU1 point, large enough simulated SM samples are needed to properly evaluate the impact on invariant mass distributions caused by background statistical fluctuations.

In order to reconstruct lepton-lepton-jet invariant mass, the two highest transverse momentum jets in the event are selected. In about 80% of signal events one of these two jets originates from $\tilde{q}_L$ decay. Two invariant masses are reconstructed on event by event basis: the larger lepton-lepton-jet invariant mass $m(jll)^{high}$ and the smaller lepton-lepton-jet invariant mass $m(jll)^{low}$, then the two jets are labelled *high* and *low* accordingly. SFOS-OFOS subtraction is applied on both mass distributions. Larger and smaller lepton-lepton-jet invariant masses are added together to get $m(jll)$, presented in Fig. 11 for the SU1 and SU3 points with the SM background superimposed.

Events in which dilepton invariant mass and larger lepton-lepton-jet invariant mass satisfy the conditions

- $m(ll) < 100$ GeV, $m(jll) < 615$ GeV (for the SU1 point),
- $m(ll) < 100$ GeV, $m(jll) < 500$ GeV (for the SU3 point),

are retained and used for further study.

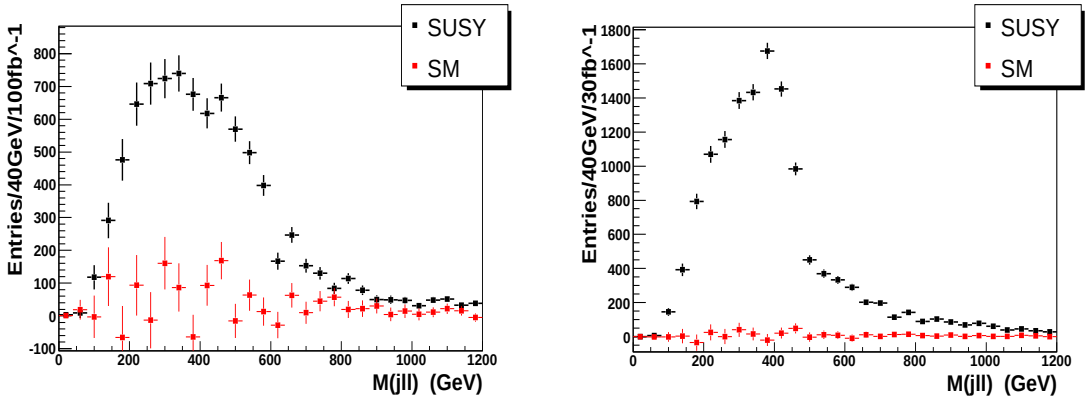

Fig. 11: Lepton-lepton-jet invariant mass formed with both jets after SFOS-OFOS subtraction for SUSY events (in black: SU1 on the left, SU3 on the right) and for SM events (in red).

	Efficiency (SU1)	S/B (SU1)	Efficiency (SU3)	S/B (SU3)
Signal	(17.0 ± 0.3) %	/	(20.0 ± 0.3)%	/
SUSY Background	(0.94 ± 0.01)%	0.33	(0.75 ± 0.01)%	1
$t\bar{t}$ + partons	$(2.69 \pm 0.02)\ 10^{-4}$	0.18	$(3.14 \pm 0.02)\ 10^{-4}$	0.9
W + partons	$(1.4 \pm 0.9)\ 10^{-5}$	~ 16	$(0.4 \pm 0.4)\ 10^{-5}$	~ 300
Z + partons	$(1.1 \pm 0.3)\ 10^{-5}$	$\sim$12	$(0.9 \pm 0.2)\ 10^{-5}$	$\sim$100

Table 1: Efficiencies and S/B ratios for SUSY signal and background (SU1, SU3) and for the most relevant sources of SM background ($l = e, \mu$). Contributions of SM processes for different number of parton jets in the event are all summed up for $t\bar{t}$, W and Z samples. No OFOS subtraction is applied.

Efficiencies after the whole selection are shown in Table 1. For SM background samples, efficiencies include parton shower matching and event filtering [15]. No SFOS-OFOS subtraction is applied in this case. The largest contribution to background is given by SUSY events, while the hardest SM background process is represented by $t\bar{t}$ + 2 or more partons, especially for SU1. After SFOS-OFOS subtraction the contribution of SUSY background to the finally selected sample is furtherly reduced by a factor $\sim$ 2, and SM processes with two uncorrelated leptons become compatible with zero within errors.

Similarly to $m(jll)$, also lepton-jet invariant mass has been computed with both high and low jets, providing $m(jl)^{low}$ and $m(jl)^{high}$, which have been added together to obtain $m(jl)$ distribution.

For the SU1 point, four lepton-jet invariant masses have been reconstructed: $m(jl^{near})_L$ and $m(jl^{far})_L$, formed with jet and near lepton or jet and far lepton, re-

spectively, in the case of $\tilde{\chi}_2^0 \rightarrow \tilde{l}_L\, l$ decay in (3.1) and $m(jl^{near})_R$ and $m(jl^{far})_R$ for the corresponding cases of $\tilde{\chi}_2^0 \rightarrow \tilde{l}_R\, l$. Decays (3.1) with $\tilde{l}_L$ or $\tilde{l}_R$ are distinguished according to the value of the dilepton invariant mass:

- $m(ll) < 57$ GeV for the $\tilde{l}_L$,
- 57 $GeV < m(ll) <$ 100 GeV for the $\tilde{l}_R$.

The selection of the decay chain which involves the $\tilde{l}_L$ is affected by a contamination (of $\sim 15\%$) due to the events with $\tilde{l}_R$ in which $m(ll) < 57$ GeV. On the other hand, the right-handed slepton selection suffers from the presence of the Z peak. Near and far leptons in both decays are selected according to their transverse momenta: in decay (3.1) with $\tilde{l}_L$, the near (far) lepton is the one with lower (higher) transverse momentum, and vice versa for the decay (3.1) with $\tilde{l}_R$. For the SU3 point there is no possibility to distinguish near and far lepton. Examples of lepton-jet invariant mass distribution are reported in Fig. 12 after SFOS-OFOS subtraction.

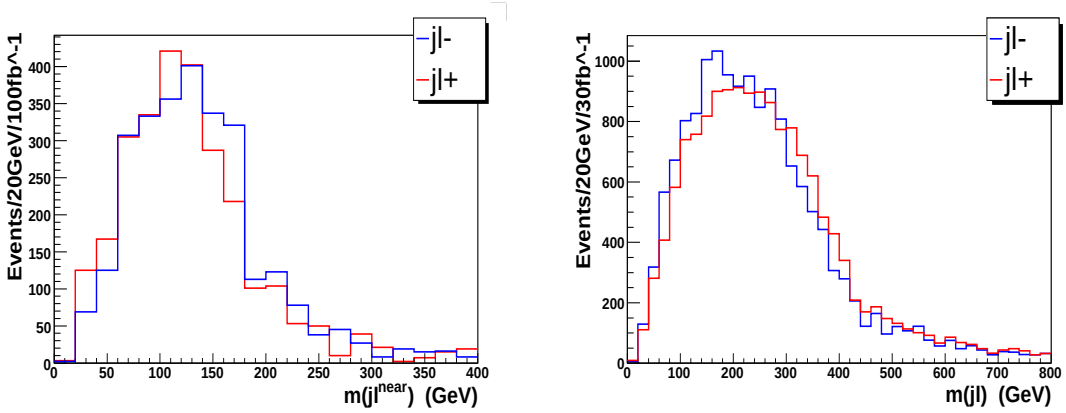

Fig. 12: Lepton-jet invariant mass distributions after SFOS-OFOS subtraction. Left: using the near lepton from the chain involving $\tilde{l}_L$ in SU1 point. Right: using both near and far leptons in SU3 point.

Summing together lepton-jet invariant masses formed with high and low jets introduces a diluting effect on charge asymmetry, since in every event (at least) one of the two jets is *wrong*, i.e. it is not associable to the quark [1] in the decay of interest, because coming from other decay chains in the event or because badly reconstructed. As will be shown in Sect. 6, the (unavoidable) choice of considering a wrong jet per event gives actually no contribution in the final charge asymmetry plots.

[1]Here a jet is said to be correctly associated to a quark if it is reconstructed within a cone of size $\Delta R = \sqrt{(\Delta\varphi)^2 + (\Delta\eta)^2} < 0.1$ around it.

6 Results and background effects on asymmetries

Charge asymmetries have been computed from the $m(jl)$ distributions shown above. OFOS entries have been statistically subtracted to SFOS entries before computing the asymmetries bin by bin. A suitable choice of the bin width has been made for each asymmetry plot in order to find a compromise between a good granularity in $m(jl)$ and a proper statistical treatment of the asymmetry and its error. Any dependence of results on the choice of the binning has been also checked and found to be negligible. Also the range over which statistical tests have been performed on $m(jl)$ charge asymmetries has been chosen to be slightly larger than the expected and observed endpoint of each lepton-jet invariant mass: this has been done in order to take into account for smearing effects on $m(jl)$ due to resolution effects, jet misidentification, etc. In the following studies on $m(jl)$ charge asymmetries, the ranges $[0, 220]$ GeV for SU1 (only for decay (3.1) with left-handed slepton and near lepton) and $[0, 420]$ GeV for SU3 point have been considered.

Two different methods have been applied in order to detect and estimate the presence of a non-zero charge asymmetry:

a. a comparison of asymmetry plots to a costant zero function $y = 0$ (hypothesis of symmetry); a non parametric χ^2 test provides a confidence level CL_{χ^2},

b. a *Run Test* method [20] for which, in order to claim for a non-zero asymmetry, only a small number of runs [2] have to be found with respect to the number of bins. A confidence level CL_{RT} for the hypothesis of no asymmetry is suitably defined, related to both the number of runs and of bins.

Methods **a** and **b** are independent and their probabilities can be combined (see for instance [20]) providing a final confidence level CL_{comb}. These tests do not depend on the original shape of the eventual charge asymmetry.

It should be remarked that the discussed methods aim at rejecting the *null* hypothesis of a zero asymmetry (or, equivalently, of invariant masses $m(jl^+)$ and $m(jl^-)$ shaped according to the same distribution).

In Fig. 13 charge asymmetries are reported for $m(jl^{near})_L$ in SU1 point and for $m(jl)$ in SU3 point, together with the confidence levels obtained with the two methods separately and combined. A horizontal line at 0 is also drawn as a reference (showing the null hypothesis). A value of CL_{comb} well below 1% is obtained for the SU1 point with 100 fb^{-1}, while 30 fb^{-1} are sufficient to get a very low confidence level ($< 10^{-9}$) in the case of the SU3 point.

As expected and already observed at MC truth level (see Sect. 4.2), charge asymmetry in the decay (3.1) with $\tilde{l}_L$ (SU1 point) is characterised by negative (positive) values for large (low) lepton-jet invariant masses, while the opposite holds when the $\tilde{l}_R$ is involved (SU3 point).

[2] A run is defined here as a set of consecutive points of the same sign, i.e. positive or negative, in the asymmetry plot.

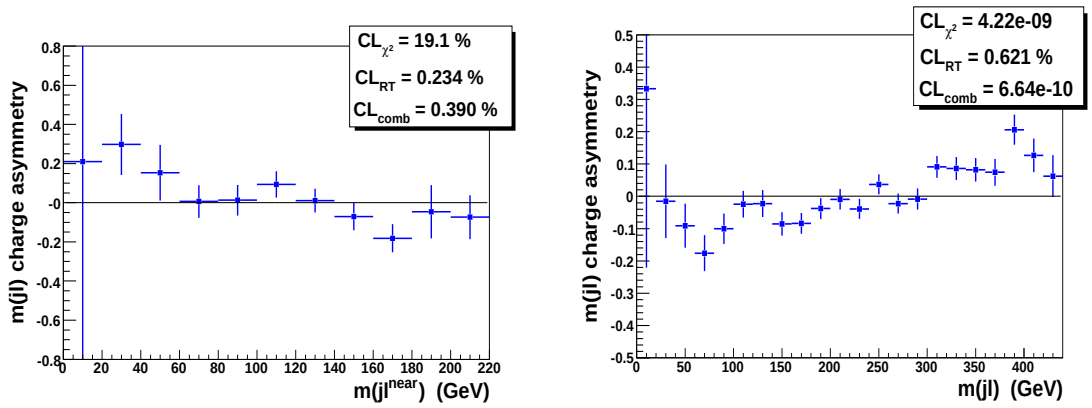

Fig. 13: Charge asymmetries for lepton-jet invariant masses after SFOS-OFOS subtraction. Left: using the near lepton from the chain involving $\tilde{l}_L$ in SU1 point. Right: using both near and far leptons in SU3 point.

As already discussed, subtracting OFOS entries to the initial $m(jl)$ SFOS distributions has the advantage of statistically removing the contribution of the reducible SFOS background. To prove that this procedure does not affect the observability of a non-zero charge asymmetry, confidence levels are calculated also starting from the $m(jl)$ distributions in all the selected OFOS events, as illustrated in Fig. 14 for SU1 and SU3 points. The combined confidence level measured in both cases is

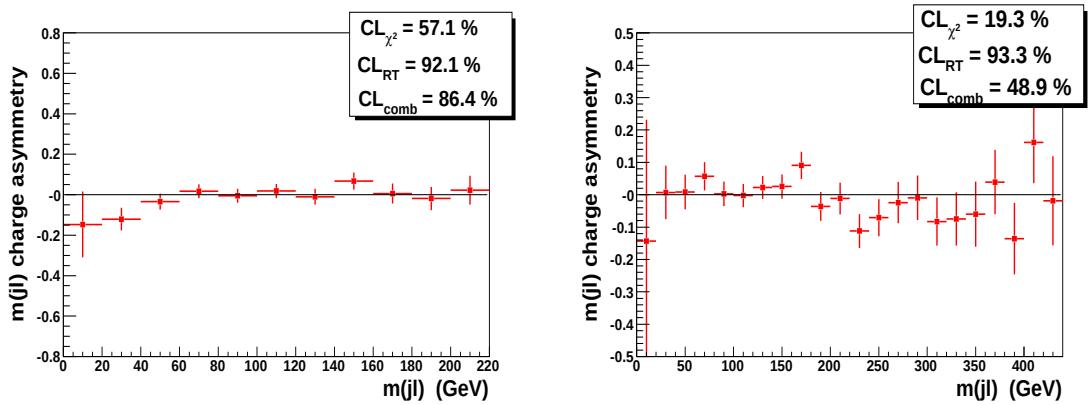

Fig. 14: Charge asymmetries for $m(jl)$ obtained in SUSY events with OFOS leptons pairs. Left: using the near lepton from the chain involving $\tilde{l}_L$ in SU1 point. Right: using both near and far leptons in SU3 point.

larger than 50%, giving quantitative evidence for the flatness of the plots.

Another test against background is given in Fig. 15, where in both SU1 and SU3 samples the charge asymmetries have been reported for SFOS background events

only: although their contribution to the final event selection is not negligible (as already reported in Table 1), they don't introduce significant biases in the charge asymmetry, as the observed CL_{comb} is high compared to the whole selected final sample including signal.

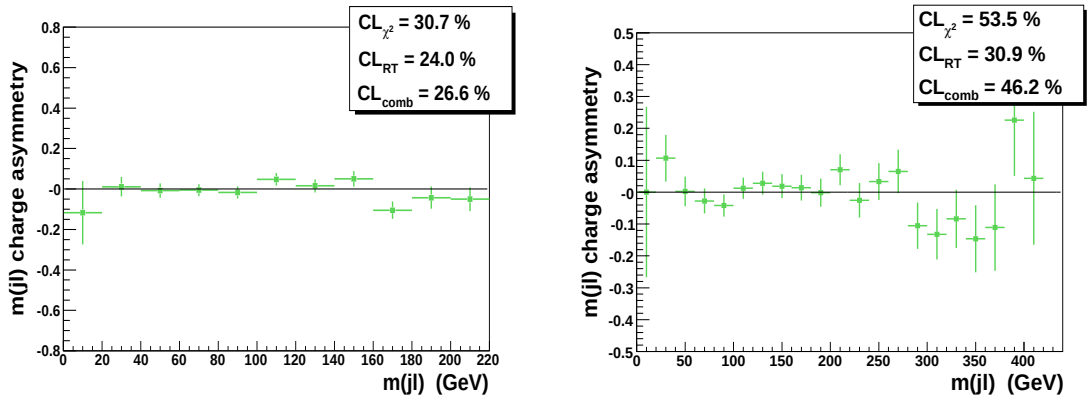

Fig. 15: Charge asymmetries for $m(jl)$ distributions obtained considering only the selected SUSY background events. Left: using the near lepton from the chain involving $\tilde{l}_L$ in SU1 point. Right: using both near and far leptons in SU3 point.

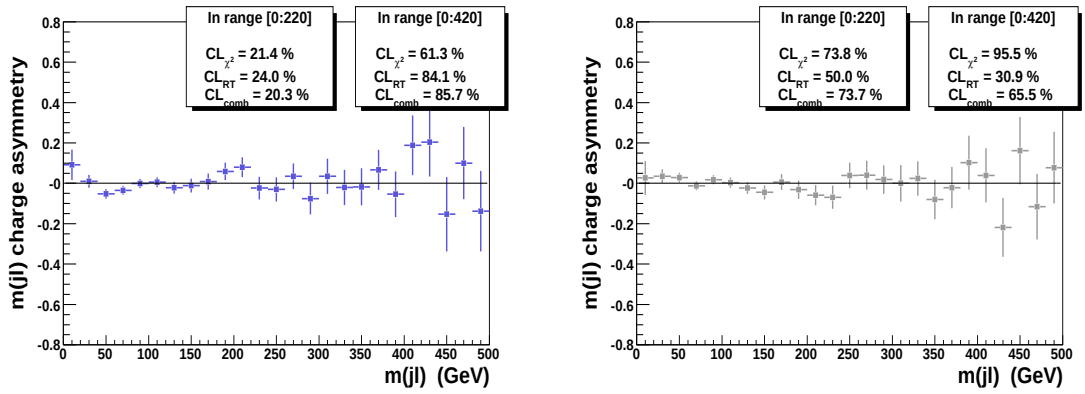

Fig. 16: Charge asymmetries for $m(jl)$ distributions of SM background events, for SFOS leptons (on the left) and for OFOS leptons (on the right).

As far as Standard Model background is concerned, charge asymmetry has been tested on both SFOS and OFOS selected events over different $m(jl)$ ranges: Fig. 16 reports the confidence level results in the range $[0, 220]$ GeV for $m(jl^{near})_L$ and in $[0, 420]$ GeV for $m(jl)$ with near and far leptons, in SU1 and in SU3 points, respectively. While CL_{comb} is usually observed to be higher than 60-70%, in the most critical condition (i.e. for $m(jl^{near})_L$ charge asymmetry in SFOS events of

SU1 point) it is approximately 20%. This scenario is in fact also critical because of the rather small $m(jl)$ range (and consequently low number of points) over which the asymmetry should be tested against accidental background fluctuations at a given integrated luminosity.

As a further check on charge asymmetry, only lepton-jet invariant masses formed with the wrong jet have been isolated on the basis of MC truth. They are shown in Fig. 17 for both SUSY points. SU3 point looks to be the most affected point,

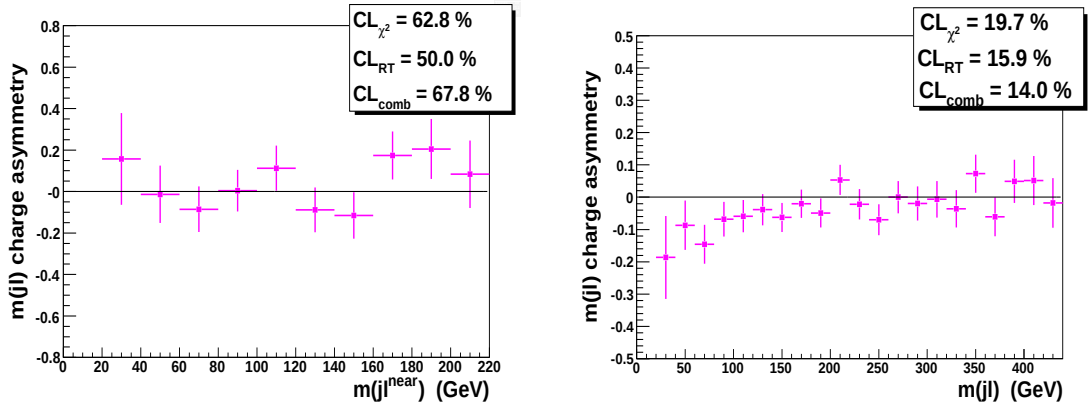

Fig. 17: Charge asymmetries for $m(jl)$ distributions obtained when a wrong jet is selected, according to MC truth. Left: using the near lepton from the chain involving $\tilde{l}_L$ in SU1 point. Right: using both near and far leptons in SU3 point.

but the apparently low confidence level for having no charge asymmetry is actually many orders of magnitude larger than what is observed when the first two jets are both used to form $m(jl)$, regardless they are wrong or correct (Fig. 13).

Finally, the effect of leptons from hadronic particles or jets misidentified as isolated leptons on charge asymmetry has been evaluated observing the sensitivity of the confidence levels to such contamination for different scenarios, as already described in Sect. 4.1. This effect, even in the worst case (i.e. simulating a contamination three times larger than that obtained with ATLFAST), produces only a negligible increase in the confidence levels, thus not spoiling the capability to observe charge asymmetry.

The whole analysis described so far has been repeated for different values of integrated luminosity: in Fig. 18 the confidence levels obtained with methods **a**, **b** and with their combination are plotted versus the integrated luminosity.

Concerning SU1 point, the evidence with a 99% confidence level for a charge asymmetry would need an integrated luminosity of at least 100 fb^{-1}, while in SU3 point $m(jl^{\pm})$ distributions can be excluded to be equal with a high probability already with less than 10 fb^{-1}.

All studies performed for this analysis are based on fast simulation samples, for which a parameterised detector response is used while, for a more detailed study,

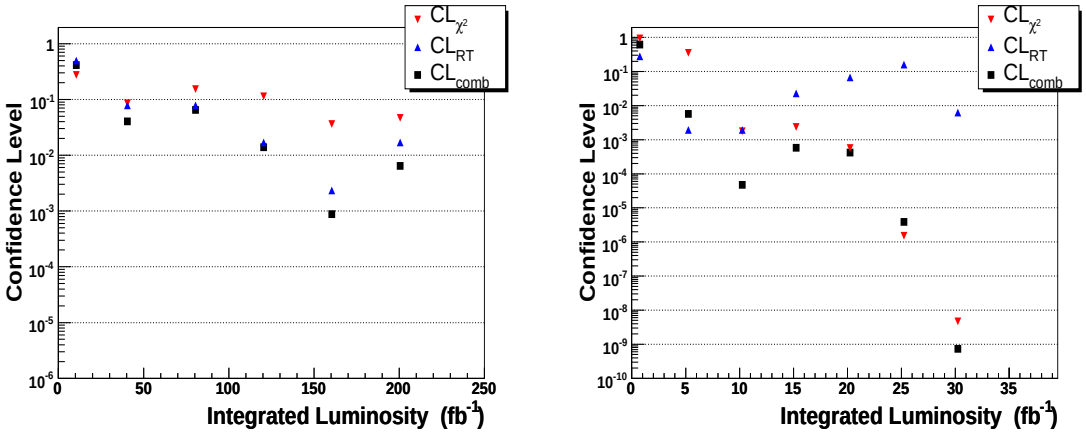

Fig. 18: Confidence levels for having no charge asymmetry in $m(jl)$ distributions as functions of integrated luminosity. Left: using the near lepton from the chain involving $\tilde{l}_L$ in SU1 point. Right: using both near and far leptons in SU3 point.

full simulation samples based on realistic detector description are needed for both SUSY and SM background with sufficient statistics (higher than the one presently available).

7 Conclusions

After a possible initial discovery of Supersymmetry at LHC, one of the main goals will be to measure properties, like spin, of newly discovered particles. In particular, the decay chain $\tilde{q}_L \rightarrow \tilde{\chi}_2^0 q \rightarrow \tilde{l}_{L,R}^{\pm} l^{\mp} q \rightarrow l^+ l^- q\ \tilde{\chi}_1^0$ has been studied in order to verify the consistency of the spin-0 slepton and spin-1/2 neutralino hypothesis, by looking for charge asymmetry in invariant mass distributions. Two recently selected SUSY points in agreement with latest experimental and theoretical constraints were considered: a "typical" mSUGRA point in the bulk region (SU3) and, as a more complicated case, a point in the stau-coannihilation region (SU1).

By applying a set of optimised cuts, the decay chain of interest was isolated and both Standard Model and SUSY background events were successfully reduced. Two independent statistical methods were used to detect the presence of charge asymmetry in invariant mass distributions. The residual background contributions were proved to have zero asymmetry and not to significantly spoil the asymmetry of the signal. Stability and consistency of the used methods have been also tested against some sources of systematics, such as wrong jet association and binning effects.

Results show that, in the fast simulation approach as the one investigated in this report without taking into account systematic effects coming from a realistic detector description, an integrated luminosity of at least 100 fb^{-1} is needed in the case of the SU1 point to observe a non-zero charge asymmetry with a confidence level of about 99%, while in the more favorable case of the SU3 point 10 fb^{-1} would

be sufficient.

8 Acknowledgements

This work has been performed within the ATLAS Collaboration, and the authors wish to thank collaboration members, and particularly Giacomo Polesello, Frank Paige, Dan Tovey and Shoji Asai for many precious suggestions and helpful discussions. The physics analysis framework and tools used in this work are the result of collaboration-wide efforts.

References

[1] S. P. Martin, hep-ph/9709356.

[2] J. Ellis, K. A. Olive, Y. Santoso and V. C. Spanos, *Phys. Lett.* **B565** (2003) 176-182, [hep-ph/0303043].

[3] A. J. Barr, *Phys.Lett.* **B596** (2004) 205-212, [hep-ph/0405052].

[4] A. Datta, K. Kong and K. T. Matchev *Phys.Rev.* **D72** (2005) 096006, [hep-ph/0509246].

[5] J. M. Smillie and B. R. Webber, *JHEP* **10** (2005) 069, [hep-ph/0507170].

[6] P. Richardson, *JHEP* **11** (2001) 029.

[7] B.C. Allanach and F. Mahmoudi, *Proc. of Les Houches "Physics at TeV Colliders 2005" beyond the SM working group: summary report* (2005) 024, [hep-ph/0602198].

[8] B.C. Allanach et *et al.*, *JHEP* **09** (2000) 004.

[9] G. Corcella *et al.*, *JHEP* **0101** (2001) 010, [hep-ph/0011363].

[10] S. Moretti *et al.*, *JHEP* **0204** (2002) 028, [hep-ph/0204123].

[11] G. Corcella *et al.*, hep-ph/0210213.

[12] Program and its documentation are available from www.hep.phy.cam.ac.uk/∼richardn/HERWIG/ISAWIG/

[13] H. Baer *et al.*, hep-ph/0001086.

[14] https://twiki.cern.ch/twiki/bin/view/Atlas/RomeSUSYWiki

[15] https://twiki.cern.ch/twiki/bin/view/Atlas/AtlFastProduction

[16] M.L. Mangano, M. Moretti, F. Piccinini, R. Pittau and A. Polosa, *JHEP* **0307** (2003) 001 , [hep-ph/0206293].

[17] E. Richter-Was, D. Froidevaux and L. Poggioli, *ATLAS Internal Note* **ATL-PHYS-98-131** (1998).

[18] B.K. Gjelsten, D.J. Miller and P. Osland, *JHEP* **12** (2004) 003, *ATLAS Note* **ATL-PHYS-2004-029** (2004).

[19] O. Jinnouchi, S. Asai, K. Oe and J. Tanaka, *ATLAS Communication* **ATL-COM-PHYS-2006-044** (2006).

[20] A.G. Frodesen, O. Skjeggestad, H. Tofte, Probability and Statistics in Particle Physics, Bergen, Norway: Universitetsforlaget (1979)